NIH Public Access
Author Manuscript
J Neurochem. Author manuscript; available in PMC 2011 August 1.

Published in final edited form as:
J Neurochem. 2010 August ; 114(3): 909–920. doi:10.1111/j.1471-4159.2010.06823.x.

Activity- and age-dependent modulation of GABAergic neurotransmission by System A-mediated glutamine uptake

Molly N. Brown and **Gregory C. Mathews**
Departments of Neurology and Pharmacology, Vanderbilt University, Nashville, Tennessee, USA

Abstract

GABAergic neurotransmission adapts to maintain normal brain function in a wide range of activity states through multiple mechanisms; presynaptic control of quantal size has only recently gained recognition as one of those mechanisms. GABA synthesis from glutamate is coupled with vesicular packaging, and therefore the supply of glutamate can affect inhibitory synaptic strength. Because System A transporters supply glutamine to neurons, where it is converted to glutamate, we hypothesized that regulation of the activity of these transporters could alter glutamine uptake and provide a mechanism to link supply to demand for neurotransmitter GABA. In immature and mature rat hippocampus, after a period of hyperexcitability, we observed a System A-dependent enhancement of inhibitory synaptic strength along with an increase in System A activity in synaptosomes under the same conditions. Under resting conditions, System A's contribution of glutamine to synaptic GABA diminished with age, correlating with reduced SNAT1/SAT1 expression and, even more so, with its activity on synaptic membranes. We conclude that System A activity is highly regulated, by depolarization and developmental cues, to dynamically modulate GABAergic transmission. Our evidence suggests that SNAT1/SAT1 is the transporter that plays a critical role in dynamically modulating inhibition in response to metabolic demands.

Keywords

GABA metabolism; System A; SNAT1/SAT1; hippocampal development; glutamine; inhibitory neurotransmission

Introduction

Normal brain function requires that inhibitory GABAergic systems adapt to a range of activity states, and increased demand for neurotransmitter GABA must be met with increased synthesis or seizures may result (Sepkuty *et al*. 2002, Kash *et al.* 1997). Because neurons are not capable of net production of glutamate, GABA's immediate metabolic precursor, interneurons rely on a supply of glutamate to maintain GABA synthesis and vesicular filling (Bak *et al.* 2006). Glutamine, which is cycled between astrocytes and neurons, can be converted to glutamate in neurons. Therefore, substrate transporters supplying either glutamate or glutamine may play a key role in linking activity-related demand for GABA to its rate of synthesis (see Figure 2A). The sodium-coupled neutral amino acid transporters SNAT1/SAT1 and SNAT2/SAT2 comprise “System A” that mediates most neuronal glutamine uptake (Broer & Brookes 2001), but whether either one plays an active role in shaping neurotransmission has not been determined.

Corresponding author: Gregory C. Mathews, Vanderbilt University Medical Center, 6128 Medical Research Building III, 465 21st Avenue South, Nashville, TN 37232-8552, USA, Phone (615) 343-0575, gregory.mathews@vanderbilt.edu.

NIH-PA Author Manuscript
NIH-PA Author Manuscript
NIH-PA Author Manuscript

NIH-PA Author Manuscript
NIH-PA Author Manuscript
NIH-PA Author Manuscript

Some studies suggest that System A-mediated glutamine uptake contributes to neurotransmitter pools only under conditions of increased metabolic demand (Tani *et al.* 2007, Bryant *et al.* 2009, Liang *et al.* 2006). However, inhibition of System A transporters rapidly reduces vesicular GABA content in immature hippocampal interneurons under resting conditions (Fricke *et al.* 2007). Therefore, we investigated whether System A-mediated glutamine uptake is regulated in order for interneurons to adapt to increased demand for GABA. Other elements involved in GABA synthesis (see Figure 2A) could also be regulated to influence inhibitory neurotransmission; however, because a concentration of glutamine capable of saturating System A transporters is available to neurons normally (McGale *et al.* 1977, Fricke et al. 2007), we hypothesized regulation of the surface activity of System A transporters would be the primary mechanism capable of modulating glutamine supply, GABA synthesis and vesicular GABA content. Moreover, because of the critical role of GABA signaling in coordinating excitatory synapse maturation and synaptogenesis (Wang & Kriegstein 2009, Ben-Ari *et al.* 2007), we hypothesized that the role of System A transporters at inhibitory synapses also may be developmentally regulated.

Using electrophysiology in hippocampal slices in conjunction with protein expression studies and uptake assays in synaptosomes, we demonstrate that System A transporters serve both constitutive and activity-dependent roles in modulating vesicular GABA content and inhibitory synaptic strength. Synaptic depolarization up-regulates the activity of System A transporters and therefore likely underlies an activity-dependent increase in vesicular GABA content in both immature and mature hippocampus. However, because System A's basal uptake activity and its constitutive contribution to vesicular GABA content diminishes over the first two postnatal weeks, it only plays an activity-dependent role in mature hippocampus. Furthermore, our results support that these constitutive and activity-dependent roles are likely mediated by the SNAT1 subtype of System A transporters. Therefore, our results strongly support the hypothesis that the activity of SNAT1, regulated both by depolarization and by developmental cues, is the key component in a novel mechanism to dynamically link metabolic demand for GABA with vesicular GABA content and inhibitory synaptic strength.

Experimental procedures

Materials

α-(Methyl-amino) isobutyric acid (MeAIB), 3-Mercaptoproprionic acid (3-MPA), (1,2,5,6-Tetrahydropyridin-4-yl) methylphosphinic acid hydrate (TPMPA), 6,7-dinitroquinoxaline-2,3-dione (DNQX), CPG55845, and dizocilpine maleate (MK-801) were obtained from Sigma (St. Louis, MO, USA). Tetrodotoxin (TTX) was obtained from Tocris (Ellisville, MO, USA). [^{3}H]MeAIB was obtained from American Radiolabeled Chemicals. Jeffrey Erickson (LSU Health Sciences Center, New Orleans, LA) provided the rabbit polyclonal anti-SNAT1 (1:14,000) and anti-SNAT2 (1:1,000) antibodies used for western blot analysis and both antibodies have been characterized previously for specificity in rat brain (Varoqui *et al.* 2000, Yao *et al.* 2000). Additional antibodies used for western blot analysis include rabbit anti-EAAC1, 1:1000 (Alpha Diagnostic International); rabbit anti-GAT-1, 1:200 (Chemicon); mouse anti-GAD65, 1:500 (Chemicon); mouse anti-actin, 1:800,000 (Chemicon).

Preparation of hippocampal slices and patch clamp recording

Sprague Dawley rats at various ages were deeply anesthetized with isoflurane and decapitated under a protocol approved by Vanderbilt University's Institutional Animal Care and Use Committee. Hippocampi were removed and cut into 400μm sections using a vibratome (Vibratome Company, St. Louis, MO, USA) in an ice-cold oxygenated solution

NIH-PA Author Manuscript

NIH-PA Author Manuscript

NIH-PA Author Manuscript

containing (in mmol/L): sucrose 75, NaCl 87, KCl 2.5, $MgCl_2$ 7, $CaCl_2$ 0.5, NaH_2PO_4 1.25, glucose 25, and $NaHCO_3$ 25. Slices were transferred to a chamber containing artificial cerebrospinal fluid (ACSF), which contained (in mmol/L): NaCl 119, KCl 2.5, $MgCl_2$ 1.3, $CaCl_2$ 2.5, NaH_2PO_4 1, glucose 11, and $NaHCO_3$ 26.2, (pH 7.4, 290mOsm) and bubbled with 95% O_2/5% CO_2. Slices were incubated at 35°C for 30 min, then at room temperature (22-25°C) for 30 min before recording.

Patch pipettes with resistances of 3-5MΩ were filled with a solution containing (in mmol/L): cesium chloride 130, HEPES 10, EGTA 10, Na^{2+}-GTP 0.2, and Mg^{2+}-ATP 2 (pH 7.4, 290 mOsm). Lidocaine *N*-ethyl bromide (QX-314; 1 mM), which blocks Na^+ channels, was included in the solution for mIPSC recording to inhibit action potential generation. For studies investigating the effects of high K^+-induced depolarization, KCl replaced cesium chloride and QX-314 was excluded. Whole cell recordings were obtained at a holding potential of -60mV with a MultiClamp 700A amplifier (Molecular Devices Corporation, Sunnyvale, CA, USA). Access resistance was monitored throughout the experiment and data were discarded if increase was more than 20%. Slices were perfused constantly at approximately 2 mL/min with ACSF (bubbled with 95% O_2/5% CO_2). Miniature inhibitory postsynaptic currents (mIPSCs) were recorded by adding tetrodotoxin (TTX; 0.5μmol/L, sodium channel blocker), DNQX (10 μmol/L, AMPA receptor antagnoist), and MK-801 (5μmol/L, NMDA receptor antagonist) to the recording solution. All experiments were performed at 22-25°C unless otherwise indicated.

After control currents were obtained, the effects of MeAIB, TPMPA or glutamine were evaluated after a 5 minute wash-in period. For TPMPA studies, CPG55845 (300nmol/L), a $GABA_B$ receptor antagonist, was included in the perfusate to block activity of TPMPA at $GABA_B$ receptors. For studies in which glutamic acid decarboxylase was inhibited, slices were incubated for 1h in 3-MPA (1mmol/L), then transferred to the recording chamber where the perfusate contained 250μmol/L 3-MPA. For experiments evaluating the effect of hyperexcitable state (Figures 1-2), slices were exposed to 2.5mmol/L KCl-ACSF (sham) or 10mmol/L KCl-ACSF (high K^+) for 20 minutes at room temperature and then transferred to the recording chamber where the remainder of the experiment was performed at 34°C. Perfusion of slices with either sham or high K^+ ACSF continued for 10 minutes while an acceptable patch clamp recording was obtained, after which the spontaneous activity was monitored in current clamp mode for an additional 3-5 minutes (eg. Figure 1A). After this approximately 30 minute period, the perfusate for all slices (sham or high K^+) was replaced with 2.5mmol/L KCl-ACSF containing TTX, DNQX, and MK-801. Therefore, all recorded neurons had a period of at least 5 minutes after whole-cell recording configuration was achieved to allow equilibration of the intracellular and pipette solution contents prior to recording mIPSCs which would be sufficient to exclude potential variations in intracellular chloride concentration between neurons in sham and high K^+ treated slices that could have confounded our results. For studies examining the effect of TPMPA or MeAIB on mIPSCs after sham treatment or high K^+-induced depolarization, we recorded mIPSCs at one-minute, washed-in TPMPA or MeAIB for 5 minutes, and assessed the drug effects on mIPSCs recorded at ten minutes post-depolarization (see Figure 1B).

Individual mIPSCs meeting threshold criteria were detected using MiniAnalysis software (Synaptosoft, Fort Lee, NJ) and visually inspected to exclude artifacts (i.e. only single events arising from a stable baseline were used for analysis). At least 100 events were recorded from each cell in each condition, and the median was calculated. Each experiment was performed in multiple cells (‘n’) prepared from at least three animals. Effect of drug or high K^+ was evaluated using a student's paired t-test unless otherwise indicated.

NIH-PA Author Manuscript

NIH-PA Author Manuscript

NIH-PA Author Manuscript

Immunohistochemistry

Coronal sections (40 μm) were prepared from fixed postnatal day 8 and 25 Sprague-Dawley rat brains as described previously (Stafford *et al.* 2010). A mouse monoclonal anti-SNAT1 antibody (N104/37; NeuroMabs, UC Davis, like the rabbit polyclonal anti-SNAT1 antibody, recognized a 52kD band in immunoblots and its binding was blocked by preadsorption with the control peptide (data not shown). Although both anti-SNAT1 antibodies displayed similar staining patterns, the rabbit polyclonal antibody demonstrated higher background staining (Supplemental Figure 1) and therefore N104/37 was used. Free-floating sections were blocked in 4% milk then incubated for 72 hours at 4°C in primary antibody. An optimal antibody dilution of 1:1000 was determined by evaluation a range of dilutions. For secondary detection, sections were incubated in biotinylated anti-mouse IgG (1:1000, Jackson Immunoresearch, PA) for one hour at room temperature, then with avidin–biotin amplification reagent with horseradish peroxidase (Vectastain Elite ABC, Vector Laboratories, Burlingame, CA). Detection of horseradish peroxidase activity was achieved with the 3,3′-diaminobenzidine reaction.

Western Blot Analysis

Hippocampi were dissected from Sprague-Dawley rats at the postnatal day indicated, immediately frozen by dry ice, weighed, and stored at -80°C. Frozen tissue was placed in ice-cold solution (15μL/mg) containing 2% SDS and a protease inhibitor cocktail (1:1000, Sigma) and sonicated. Protein concentrations were determined using the colorimetric *DC* Protein Assay (Bio-Rad). Samples were diluted 1:1 in 2× sample buffer (0.125M Tris base, 10% SDS, 10% glycerol, 0.02% Bromophenol blue, 4% β-mercaptoethanol, pH 6.8) and stored at -80°C. Equal amounts of protein (20μg for GAT-1 experiments, 10μg for all remaining experiments) were loaded on a 10% Tris-Glycine polyacrylamide gel. After electrophoretic separation, proteins were transferred to a PVDF membrane. Membranes were blocked with 5% milk plus 0.1% Tween 20 for 1 hour at room temperature, and incubated with the respective primary antibody overnight at 4°C. After several washes in PBS plus 0.1% Tween 20, membranes were incubated in horseradish peroxidase-conjugated secondary antibodies (1:20,000, Jackson Laboratories; 1h at room temp.), washed, developed with enhanced chemiluminescence reagents (ECL kit, Amersham) and then exposed to autoradiography film. Measurements of each protein were conducted in the same sample, and all experiments were repeated in three different animals at each age. Band intensity was measured with ImageJ software. Statistical correlations between SNAT1/actin or SNAT2/actin protein expression with time were assessed using Spearman's Rank Order Correlation Test (Figure 4B) and developmental differences between the SNAT1:actin protein ratio in synaptosomes were assessed using a student's t-test (Figure 5A).

Preparation of synaptosomes and [^{3}H]MeAIB uptake assays

Crude synaptosomes were prepared by dissecting hippocampi from immature (P8-11) and mature (P21-28) Sprague-Dawley rats which were immediately immersed in 3mL of an ice-cold solution containing (in mmol/L): sucrose 320, NaCl 119, KCl 2.5, $MgCl_2$ 1.3, $CaCl_2$ 2.5, NaH_2PO_4 1, glucose 11, and HEPES 10. Tissue was homogenized (400 rpm) using a Teflon-glass tissue homogenizer (Wheaton Instruments, Millville, NJ) followed by centrifugation (2000 rpm, 10 minutes, 4°C). The supernatant was transferred to clean centrifugation tubes, centrifuged (13,000 rpm, 15 min, 4°C), their supernatants discarded and the pellet was re-suspended (1mL ACSF, 10mM HEPES replacing $NaHCO_3$) and analyzed for protein concentration (Bio-Rad protein assay reagent, 1:5). For western blot analysis, synaptosomes were diluted 1:1 in sample buffer and probed for SNAT1, GAD65, and actin according to conditions specificed above. For uptake assays, samples containing 325μg protein each were incubated (10m unless otherwise indicated) in a shaking water bath (37°C) prior to adding [^{3}H]MeAIB (2.5m; 167nmol/L; specific activity, 60Ci/mmol).

NIH-PA Author Manuscript

NIH-PA Author Manuscript

NIH-PA Author Manuscript

[^{3}H]MeAIB uptake was terminated by adding 1 mL ice-cold ACSF (choline chloride replacing NaCl). Uptake after high K^+-induced depolarization was examined according to the protocol published in Ferguson *et al.* 2003. Samples were incubated in sham (2.5mmol/L KCl) or high potassium (10mmol/L KCl) ACSF for 15 minutes in a shaking water bath (37°C). Samples were then immediately centrifuged (13,000rpm, 2m), their supernatants discarded, and the pellets were resuspended with sham ACSF. All samples incubated in a shaking water bath (37°C) for either 1 or 10 minutes prior to adding 167nmol/L [^{3}H]MeAIB (2.5m). Samples were collected onto 0.3% polyethylenimine-coated glass fiber filters and washed three times with ice-cold ACSF using a Brandel cell harvester. Filters were immersed in scintillation fluid overnight and radioactivity was counted by scintillation spectrometry. All uptake assays were performed in triplicate and specific MeAIB uptake was determined by subtracting uptake in parallel samples prepared in ACSF where choline chloride replaced sodium chloride. MeAIB uptake following high K^+-induced depolarization was normalized to the respective sham control and reported as a percent of control ± SEM. Statistical significance for both [^{3}H]MeAIB uptake experiments was assessed using a student's t-test.

Results

Hyperexcitability induces a System A-dependent increase in quantal size and synaptic cleft GABA concentration

Recent studies have demonstrated that glutamine supplied by System A transporters sustains neurotransmitter pools under conditions of increased metabolic demand (Bryant et al. 2009, Liang et al. 2006, Tani et al. 2007). Because extracellular glutamine concentration is sufficient to saturate System A transporters, we hypothesized that the activity of System A transporters plays a key regulatory role within the glutamate-glutamine-GABA (glu-gln-GABA) pathway (see Figure 2A) to meet metabolic demand. Based upon evidence that individual synaptic vesicles do not contain enough GABA to saturate postsynaptic receptors in hippocampus and that changes in vesicular GABA content influence the concentration of GABA within the synaptic cleft ($[GABA]_{cleft}$) and thereby modulate the amplitudes of mIPSCs, (Mathews & Diamond 2003, Stafford *et al.* 2010, Hartmann *et al.* 2008), we further hypothesized that alterations in System A transporter activity could dynamically regulate inhibitory synaptic transmissin.

We induced a hyperexcitable state in hippocampal slices by transiently elevating extracellular potassium, and we assessed quantal size immediately afterwards by recording mIPSCs in CA1 pyramidal neurons. Slices were exposed to ACSF containing 10mmol/L KCl (“high K^+-induced depolarization”) or control ACSF containing 2.5mmol/L KCl (“sham”) for 30 minutes. Toward the end of a 30 minute period, recordings were made in CA1 pyramidal neurons using the whole cell patch clamp technique after allowing sufficient time for equilibration of the patch pipette solution with the intracellular contents. Recording in current clamp mode in the high K+ ACSF revealed depolarization of the membrane potential by approximately 15mV and an increase in the frequency of both action potentials and postsynaptic potentials (Figure 1A) compared with sham treated slices. To measure quantal size immediately following depolarization, the perfusate was switched to control ACSF containing TTX and mIPSCs were recorded (Figure 1B). In slices from immature (P8-12) rats, mIPSC amplitudes increased from 34 ± 9 pA immediately after high K^+-induced depolarization to 41 ± 12 pA ten minutes after depolarization ($p<0.05$, n=7; Figure 1Ci). This increase is reflected in a shift in the distribution of mIPSC amplitudes toward larger amplitudes at ten minutes post-depolarization ($p<0.01$, KS test; Figure 1Cii). The increase in quantal size was due to the high K^+ as no change in mIPSC amplitudes was observed following sham treatment (p=0.3, n=4; Supp. Fig. 2). Similarly, in mature (P21-28) slices, mIPSC amplitudes were increased from 32 ± 6 pA to 39 ± 7 pA ten minutes after

NIH-PA Author Manuscript

NIH-PA Author Manuscript

NIH-PA Author Manuscript

high K^+-induced depolarization ($p<0.05$, n=7; Figure 1Di) and the amplitude distribution was shifted toward larger values ($p<0.01$, KS test; Figure 1Dii). No change in mIPSC amplitudes was observed following sham treatment (p=0.9, n=3; Supp. Fig. 2).

Since an increase in quantal size may result from either pre- or postsynaptic changes, we examined the effect of TPMPA on mIPSC amplitudes following high K^+-induced depolarization to distinguish between a change in synaptic $[GABA]_{cleft}$ and a change in post-synaptic receptor number or sensitivity. TPMPA is a weak competitive antagonist at $GABA_A$ receptors with a dissociation time constant that is more rapid than the synaptic cleft transient of GABA (Jones *et al.* 2001). As a result, the degree of antagonism by TPMPA depends on $[GABA]_{cleft}$ and therefore is sensitive to changes in vesicular GABA content (Liang et al. 2006, Hartmann et al. 2008). If the increase in quantal size following high K^+-induced depolarization were due to an elevation in $[GABA]_{cleft}$, TPMPA's efficacy should be reduced. First, we determined the concentration of TPMPA required to reduce mIPSC amplitudes by the same amount at each age following sham treatment. There was a slight difference in the concentration needed to reduce mIPSCs by 20-25% (Immature: 100μmol/L, 21 ± 4%, n=5; Mature: 85μmol/L, 26 ± 3%, n=5; Figure 1E), suggesting that, at baseline, $[GABA]_{cleft}$ decreases during postnatal maturation. In both immature and mature slices, the effect of TPMPA on mIPSC amplitudes after high K^+-induced depolarization was reduced compared with its effect after sham treatment (Immature: +4 ± 5%, $p<0.01$, n=5; Mature: -4 ± 8%, $p<0.05$, n=5; student's t-test, Figure 1E), consistent with augmented vesicle content and $[GABA]_{cleft}$ underlying the increased quantal size.

In both immature and mature slices, the increase in mIPSC amplitudes peaked at ten minutes following high K^+-induced depolarization and was followed by a return to baseline values (Immature: $p<0.01$, n=7; Mature:, $p<0.05$, n=7; Repeated Measures ANOVA, Figure 2B,C). In contrast, we observed no change in mIPSC amplitudes at any time following sham treatment (Immature: p=0.6, n=4; Mature: p=1.0, n=3; repeated measures ANOVA, Figure 2B,C). In order to determine if the increase in vesicular GABA content required System A transporter activity, we tested the effect of MeAIB, a specific inhibitor of System A transporters, on mIPSC amplitudes following high K^+-induced depolarization. With an apparent affinity of approximately 1mmol/L (Mackenzie *et al.* 2003, Yao et al. 2000), MeAIB has been used at 5–50mmol/L to selectively inhibit System A transporters in a number of *in vitro* studies (Bacci *et al.* 2002, Rae *et al.* 2003, Liang et al. 2006, Fricke et al. 2007). MeAIB (10mmol/L) blocked the increase in mIPSC amplitudes following high K^+-induced depolarization in both immature (p=0.2, n=5; Figure 2B) and mature (p=0.9, n=5; Figure 2C) slices, suggesting that the increase in vesicular GABA content required ongoing System A activity after the hyperexcitable period had ended.

A glutamine-dependent increase in synaptic GABA during periods of depolarization and increased neuronal activity could be mediated by an up-regulation of multiple elements within the glu-gln-GABA cycle (Figure 2A). However, because extracellular glutamine concentrations saturate System A transporters [(Fricke et al. 2007); see also Figure 6 below], we hypothesized that an increase in the activity of System A transporters could underlie the increase in vesicular GABA content. Therefore, we measured the uptake of [^{3}H]MeAIB after high K^+-induced depolarization compared with sham treatment (analogous conditions to the slice experiments) in synaptosomes prepared from both immature and mature hippocampus. High K^+-induced depolarization increased [^{3}H]MeAIB uptake to 183 ± 31% of control ($p<0.05$, n=7) at one minute and to 151 ± 34% (p=0.2, n=9) at ten minutes in immature synaptosomes (Figure 2D). In mature synaptosomes, [^{3}H]MeAIB uptake was increased at ten minutes after high K^+-induced depolarization to 206 ± 43% ($p<0.05$, n=5; Figure 2E). Therefore, depolarization of synaptic membranes increased System A activity within the time frame when augmentation of mIPSC amplitudes was observed in intact

NIH-PA Author Manuscript

NIH-PA Author Manuscript

NIH-PA Author Manuscript

slices, although a significant change in synaptosomal uptake was observed earlier than the change in mIPSC amplitudes in the immature hippocampus.

System A glutamine uptake contributes constitutively to synaptic GABA in an age-dependent manner

When examining the effect of MeAIB on mIPSCs in immature hippocampus (Figure 2B), we observed that MeAIB reduced quantal size below baseline in both control and high K^+-induced depolarization conditions. The effect under control conditions is consistent with our previously report demonstrating a constitutive contribution of glutamine to filling of synaptic vesicles with GABA, and these studies were performed in immature hippocampi (Fricke et al. 2007). In this study, we did not see a similar effect of MeAIB on baseline mIPSC amplitudes in the mature hippocampi (Figure 2C), suggesting the possibility of a differential constitutive contribution of glutamine to synaptic GABA across development. Therefore, we examined the effect of MeAIB (10mmol/L) on mIPSC amplitudes in resting conditions at sequential postnatal ages. In immature slices, MeAIB rapidly reduced mIPSC amplitudes, consistent with a constitutive contribution of glutamine by System A transporters for vesicular GABA synthesis (Figure 3). However, over the second postnatal week, the effect of MeAIB diminished and was absent in mature slices ($p<0.05$; Figure 3).

We considered the possibility that during maturation, System A-dependent glutamine uptake could become restricted to a subpopulation of inhibitory neurons, and because mIPSCs are derived from the entire population of inhibitory synapses, a restricted effect might not be detected. To address this possibility, we assumed that subpopulations of synapses would contribute mIPSCs of similar amplitudes and therefore we analyzed the amplitudes by quartiles. We found that MeAIB uniformly reduced mIPSC amplitudes in each quartile in immature slices (P7-8; $p<0.05$ in each quartile), and mIPSC amplitudes were not reduced in any quartile in mature slices (data not shown), arguing against a restricted effect of MeAIB. We also considered that if MeAIB reduced the probability of vesicle release or altered postsynaptic membrane properties, these “non-specific” effects could somehow be age-dependent. However, we did not observe a correlation between postnatal age and either mIPSC frequency ($p=0.5$) or mIPSC decay time constant ($p=0.8$) in the presence of MeAIB (Supplementary Table 1). Therefore, the most likely explanation for the age-dependent reduction in MeAIB's effect is a uniform loss of the contribution of System A-dependent glutamine uptake to mature inhibitory synapses.

An age-dependent change in System A activity at inhibitory synapses correlates with the loss of glutamine's contribution to vesicular GABA

To test the hypothesis that there is an age-dependent loss in the constitutive activity of System A transporters, we assayed both their expression and the activity. We focused on SNAT1 given recent evidence that SNAT2 is selectively expressed by excitatory neurons in hippocampus (Gonzalez-Gonzalez *et al.* 2005, Jenstad *et al.* 2009). We found that SNAT1 was expressed selectively in a population of non-pyramidal neurons in area CA1, and that this pattern was indistinguishable between immature and mature hippocampus (Figure 4A). Next we measured total SNAT1 in whole hippocampal lysates at sequential postnatal ages using a semiquantitative Western blot approach. SNAT1 protein was highly expressed in immature hippocampus, and gradually decreased throughout postnatal development to adult levels ($p<0.001$, $n=3$; Figure 4B), paralleling the age-dependent loss of System A's constitutive contribution of glutamine to synaptic GABA (Figure 3). In contrast to SNAT1, the immature hippocampus expressed a low amount of SNAT2 protein that was higher in adult hippocampus ($n=3$; Figure 4C). Because SNAT1 expression appeared restricted to interneurons, we considered the level of glutamic acid decarboxylase 65 (GAD65, the synaptic isoform of GAD) to be a more relevant comparison for the age-dependent change

NIH-PA Author Manuscript

NIH-PA Author Manuscript

NIH-PA Author Manuscript

in SNAT1 expression. In agreement with the reported increase in number of hippocampal GABAergic synapses during the first three postnatal weeks (Danglot *et al.* 2006), we found that GAD65 expression gradually increased (Figure 4B). When we examined the ratio of SNAT1 to GAD65, there was an approximately 25-fold decrease in the expression of SNAT1 relative to GAD65 at P25 compared with P8 (data not shown).

We also examined the expression profile of two additional transporters involved in synaptic GABA metabolism: the excitatory amino acid transporter, EAAT3 (see Figure 2A), and the GABA reuptake transporter, GAT-1, to determine if SNAT1 expression is uniquely regulated during development. The relative expression ratio for each transporter displayed a different temporal pattern (Supp. Figure 3), supporting a highly specific age-dependent regulation of SNAT1 expression by inhibitory neurons.

These findings demonstrate that SNAT1 in the hippocampus is expressed selectively by interneurons and that a decrease in SNAT1 expression during a period of inhibitory synaptogenesis correlates with a loss of System A's constitutive contribution of glutamine to synaptic GABA. We hypothesized that the physiologically-relevant pool of System A transporters would be enriched in the synaptosomes, and that age-dependent changes in SNAT1 protein would be even more pronounced in this fraction than in whole hippocampal lysates. As expected, immature synaptosomes expressed an increased amount of SNAT1 protein relative to mature synaptosomes ($p<0.01$, n=3; Figure 5A). In addition, the proportional difference in amount of SNAT1 protein expressed between immature and mature hippocampus was magnified in the synaptosomal fraction (2.7 ± 0.6 fold higher) compared with the whole lysate (1.8 ± 0.4 fold higher; compare Figure 4B with Figure 5A), supporting a greater reduction in the physiologically-relevant pool. To further investigate whether SNAT1 basal uptake activity correlated with its protein levels, we measured uptake of [^{3}H]MeAIB in immature and mature hippocampal synaptosomes. After a 2.5 minute incubation, basal [^{3}H]MeAIB uptake was almost four-fold higher in immature compared with mature synaptosomes ($p<0.05$, n=3; Figure 5B) and this difference was conserved with both 5 and 10 minute incubations of [^{3}H]MeAIB (data not shown). Although MeAIB is a substrate for both SNAT1 and SNAT2, the developmental decrease in SNAT1 protein expression in synaptosomes is reflected in a parallel reduction in MeAIB uptake, and therefore interneuron terminals likely selectively reduce SNAT1 uptake activity in an age-dependent manner. Therefore, we conclude that SNAT1 protein expression and, even more so, its activity at inhibitory synapses is developmentally regulated and likely governs the age-dependence of System A's constitutive contribution to synaptic GABA.

Other elements in the GABA substrate supply pathway do not undergo age-dependent changes

Although glutamine uptake appears to be the key regulatory point in the glu-gln-GABA pathway at synapses, we considered that developmental structural changes in the hippocampus, particularly in the relationships between inhibitory synapses and astrocytic processes or excitatory synapses could also result in changes in substrate (glutamine or glutamate, respectively) availability (see Figure 2A). To address this possibility, we examined if a decrease in glutamine supply upstream or a decrease in the contribution of new GABA synthesis to vesicular filling downstream of System A transporters could explain the age-dependent loss of System A's constitutive contribution of glutamine to synaptic GABA.

We first investigated potential changes in glutamine supply by examining the effect of exogenous L-glutamine on mIPSC amplitudes. We confirmed our previous report that addition of exogenous L-glutamine (2mmol/L) had no effect on mIPSC amplitudes in immature hippocampal slices, arguing that endogenous extracellular glutamine levels

NIH-PA Author Manuscript

NIH-PA Author Manuscript

NIH-PA Author Manuscript

already saturate System A transporters ((Fricke et al. 2007), Figure 6A, B). Therefore, if endogenous extracellular glutamine were sufficiently reduced in mature hippocampus such that glutamine no longer constitutively contributed to synaptic GABA, then addition of exogenous L-glutamine should increase mIPSC amplitudes. However, exogenous L-glutamine had no effect on mIPSC amplitudes in mature slices either (101 ± 5% of control, n=5, p=0.8; Figure 6A,B). Next, we investigated if mature synaptic vesicles rely less on newly synthesized GABA for vesicle filling by comparing the effect of the GAD inhibitor, 3-mercaptoproprionic acid (3-MPA), on mIPSC amplitudes from immature and mature slices. If newly synthesized GABA is not required for vesicle filling in mature neurons, inhibiting GAD should have no effect on mIPSC amplitudes. However, 3-MPA (1mmol/L) reduced mIPSC amplitudes to a similar extent in immature and mature slices (Immature: 35 ± 9 pA, n=10 vs. 25 ± 7 pA after 3-MPA, $p<0.05$, n=7; Mature: 36 ± 5 pA, n=18 vs. 30 ± 5 pA after 3-MPA, $p<0.05$, n=5; student's t-test, Figure 6C,D). These results support that a decrease in System A-mediated glutamine uptake, and not other elements of the glu-gln-GABA pathway, mediates the age-dependent loss of System A's constitutive contribution of glutamine to synaptic GABA.

Discussion

Coupling between GABA synthesis and vesicle filling (Jin *et al.* 2003) provides a mechanism whereby supply of GABA's metabolic precursors to inhibitory synapses may dynamically up- or down-regulate vesicular GABA content and quantal size. Although dynamic changes in vesicle content are a newly recognized form of synaptic plasticity (Edwards 2007), there are very few examples where this plasticity is observed under physiological conditions. We now have demonstrated that an increase in metabolic demand results in both a System A-dependent enhancement of inhibitory synaptic strength along with an increase in System A activity in synaptosomes. These findings support that the activity of System A transporters is acutely regulated to modulate inhibitory quantal size. We also have demonstrated that the constitutive contribution of System A-mediated glutamine uptake to synaptic GABA is determined by a developmentally regulated change in the activity of these transporters, paralleling a maturational change in the role of GABA in the hippocampus.

We showed previously that uptake of exogenous (Mathews & Diamond 2003) or synaptically released (Stafford et al. 2010) glutamate by EAAT3 enhances quantal size (see Figure 2A). However, because astrocytes maintain very low extracellular glutamate levels, this metabolic pathway may only contribute to synaptic GABA under conditions in which extracellular glutamate overwhelms astrocytic glutamate transporters. In contrast, extracellular glutamine is high enough to provide a continuous supply to inhibitory synapses. Of the two independent substrate supply pathways (EAAT3 and System A), the System A pathway appears to be regulated intrinsically through transporter activity rather than substrate availability, and likely plays a unique role in homeostatic plasticity of inhibitory synapses.

SNAT1 is a key regulator of GABA metabolism at inhibitory synapses

Although both System A transporters, SNAT1 and SNAT2, have been viewed traditionally as potential suppliers of glutamine for synaptic glutamate and GABA (Bak *et al.* 2006), recent immunohistochemical studies indicate that these two transporters have distinct and non-overlapping expression patterns in the hippocampus. SNAT2 is selectively expressed by excitatory neurons in adult hippocampus (Jenstad *et al.* 2009, Gonzalez-Gonzalez *et al.* 2005), and does not appear to play a significant role in neurotransmitter glutamate metabolism (Kam & Nicoll 2007, Grewal *et al.* 2009). In contrast, our immunohistochemical findings are supported by a recent study demonstrating SNAT1

NIH-PA Author Manuscript

NIH-PA Author Manuscript

NIH-PA Author Manuscript

protein expression limited to GAD67-expressing neurons in area CA1 (Solbu *et al.*). This study also demonstrated co-localization of SNAT1 protein with the vesicular GABA transporter (vGAT), a marker for GABAergic presynaptic terminals, at axon varicosities in cortical interneuron-enriched cultures. Moreover, in our study, SNAT2 protein actually increased with age (Figure 4), opposite to the electrophysiological and biochemical studies showing a maturational loss in System A's constitutive contribution of glutamine to synaptic GABA (Figure 3). Although we did not rule out a role for SNAT2 in neurotransmitter GABA metabolism, we have provided multiple lines of evidence implicating SNAT1. Therefore, although the synaptic localization of SNAT1 has been controversial previously (Melone *et al.* 2004), our current study and that of Solbu et al. strongly support the conclusion that SNAT1 functions at or near inhibitory synaptic terminals to supply glutamine for neurotransmitter synthesis.

Activity-dependent regulation of System A surface activity modulates vesicular GABA content

Our study is the first to demonstrate dynamic modulation of inhibitory synaptic strength via regulation of the activity of a presynaptic substrate transporter. Because our findings show that extracellular glutamine levels are sufficient to saturate System A transporters, altering glutamine supply to inhibitory synapses requires up- or down-regulation of their activity. Previous studies in mature animals were able to demonstrate a requirement for glutamine to maintain neurotransmitter pools only during periods of increased metabolic demand (Bryant et al. 2009, Liang et al. 2006, Tani et al. 2007). Whether specific elements involved in the cycling of glutamine between astrocytes and neurons can be up-regulated had not been previously explored. However, our results show that inhibitory neurons adapt to an increase in metabolic demand by up-regulating System A activity, offering a mechanism for increasing GABA synthesis.

Several studies have demonstrated that hyperexcitability and acute seizure-like activity can be induced in hippocampal slices by elevating extracellular potassium (Jensen & Yaari 1997, Dzhala & Staley 2003). We induced a more moderate level of hyperexcitability with the goal of depolarizing neurons, increasing synaptic activity and creating a higher demand for GABA. After 30 minutes, quantal size at GABAergic synapses was transiently increased. Interestingly, the increase in quantal size was delayed, appearing within 10 minutes after the depolarization. There are two possible explanations for this finding: One explanation is that although System A activity is increased during the period of hyperexcitability, other factors explain why quantal size does not increase until after membrane potential or level of synaptic activity returns to normal. For example, System A activity could increase to maintain GABA synthesis and vesicular filling during the hyperexcitable state, compensating for increased demand. When synaptic activity is halted abruptly by addition of tetrodotoxin, the higher rate of GABA synthesis and slower rate of vesicular release may result in an “overfilling” of vesicles. In this case, up-regulation of System A may serve only to maintain, not to enhance, quantal size in the face of increased demand. Alternatively, elevated K^+ could impair the function of System A transporters due to reduction of the electrochemical gradient driving glutamine uptake such that an increase in glutamine uptake occurs only when a normal gradient is restored.

The second explanation is that there is a delay in the upregulation in System A activity in response to depolarization. For example, it may take minutes for biochemical signals to translate into increased surface activity, although the precise mechanism of transporter regulation and the signals involved have not been determined. The mechanism may involve either regulation of System A's catalytic efficiency or translocation of transporters to the surface, or both. In the immature synaptosomes, System A activity was increased immediately following depolarization, whereas in the mature synaptosomes, the increase

NIH-PA Author Manuscript

NIH-PA Author Manuscript

NIH-PA Author Manuscript

was observed after a delay. Differences in the preparations (slices vs. synaptosomes) may affect the sensitivity of the assays and may explain why the time course for the increase in mIPSC amplitudes differs from that of [^{3}H]MeAIB uptake. For example, some glial cells may express SNAT1 (Melone *et al.* 2004), and therefore glial membranes within the synaptosomes could contribute to the time course discrepancy. However, it remains a possibility that different mechanisms are involved in the activity-dependent role of System A transporters at different ages. Clearly, direct measurement of changes in surface expression of SNAT1 or kinetic measurements of its transport function will provide a definitive answer to this question.

Implications of altered System A activity during hippocampal maturation

Why would developing inhibitory neurons scale down the constitutive activity of System A transporters but maintain an intrinsic mechanism to increase its surface activity upon synaptic depolarization? During early postnatal development, inhibitory synapses form before excitatory synapses and therefore likely encounter little extracellular glutamate. We hypothesize System A's constitutive activity functions to sustain synaptic GABA synthesis during this period until a sufficient density of excitatory synapses is reached. The activity-dependent regulation of System A provides a supply of substrate for GABA synthesis in response to increased demand and may function throughout life to maintain a normal balance between excitation and inhibition within neuronal circuits.

Supplementary Material

Refer to Web version on PubMed Central for supplementary material.

Acknowledgments

This work was supported by NINDS grant number NS062090 (GCM) and NIGMS grant number T32GM007628 (MNB). We thank Drs. Helene Varoqui and Jeffrey Erickson for providing their SNAT1 and SNAT2 antibodies, Misty Stafford for completing the immunohistochemical experiments and Dr. Randy Blakely for help with the synaptosomal uptake assays.

References

Bacci A, Sancini G, Verderio C, Armano S, Pravettoni E, Fesce R, Franceschetti S, Matteoli M. Block of glutamate-glutamine cycle between astrocytes and neurons inhibits epileptiform activity in hippocampus. Journal of Neurophysiology. 2002; 88:2302–2310. [PubMed: 12424271]

Bak LK, Schousboe A, Waagepetersen HS. The glutamate/GABA-glutamine cycle: aspects of transport, neurotransmitter homeostasis and ammonia transfer. Journal of Neurochemistry. 2006; 98:641–653. [PubMed: 16787421]

Ben-Ari Y, Gaiarsa JL, Tyzio R, Khazipov R. GABA: a pioneer transmitter that excites immature neurons and generates primitive oscillations. Physiological Reviews. 2007; 87:1215–1284. [PubMed: 17928584]

Broer S, Brookes N. Transfer of glutamine between astrocytes and neurons. Journal of Neurochemistry. 2001; 77:705–719. [PubMed: 11331400]

Bryant AS, Li B, Beenhakker MP, Huguenard JR. Maintenance of thalamic epileptiform activity depends on the astrocytic glutamate-glutamine cycle. Journal of Neurophysiology. 2009; 102:2880–2888. [PubMed: 19741104]

Danglot L, Triller A, Marty S. The development of hippocampal interneurons in rodents. Hippocampus. 2006; 16:1032–1060. [PubMed: 17094147]

Dzhala VI, Staley KJ. Transition from interictal to ictal activity in limbic networks in vitro. J Neurosci. 2003; 23:7873–7880. [PubMed: 12944517]

Edwards RH. The neurotransmitter cycle and quantal size. Neuron. 2007; 55:835–858. [PubMed: 17880890]

NIH-PA Author Manuscript

NIH-PA Author Manuscript

NIH-PA Author Manuscript

Fricke MN, Jones-Davis DM, Mathews GC. Glutamine uptake by System A transporters maintains neurotransmitter GABA synthesis and inhibitory synaptic transmission. Journal of Neurochemistry. 2007; 102:1895–1904. [PubMed: 17504265]

Gonzalez-Gonzalez IM, Cubelos B, Gimenez C, Zafra F. Immunohistochemical localization of the amino acid transporter SNAT2 in the rat brain. Neuroscience. 2005; 130:61–73. [PubMed: 15561425]

Grewal S, Defamie N, Zhang X, De Gois S, Shawki A, Mackenzie B, Chen C, Varoqui H, Erickson JD. SNAT2 amino acid transporter is regulated by amino acids of the SLC6 gamma-aminobutyric acid transporter subfamily in neocortical neurons and may play no role in delivering glutamine for glutamatergic transmission. The Journal of Biological Chemistry. 2009; 284:11224–11236. [PubMed: 19240036]

Hartmann K, Bruehl C, Golovko T, Draguhn A. Fast homeostatic plasticity of inhibition via activity-dependent vesicular filling. PloS one. 2008; 3:e2979. [PubMed: 18714334]

Jensen MS, Yaari Y. Role of intrinsic burst firing, potassium accumulation, and electrical coupling in the elevated potassium model of hippocampal epilepsy. Journal of Neurophysiology. 1997; 77:1224–1233. [PubMed: 9084592]

Jenstad M, Quazi AZ, Zilberter M, et al. System A transporter SAT2 mediates replenishment of dendritic glutamate pools controlling retrograde signaling by glutamate. Cereb Cortex. 2009; 19:1092–1106. [PubMed: 18832333]

Jin H, Wu H, Osterhaus G, et al. Demonstration of functional coupling between gamma -aminobutyric acid (GABA) synthesis and vesicular GABA transport into synaptic vesicles. Proceedings of the National Academy of Sciences of the United States of America. 2003; 100:4293–4298. [PubMed: 12634427]

Jones MV, Jonas P, Sahara Y, Westbrook GL. Microscopic kinetics and energetics distinguish GABA(A) receptor agonists from antagonists. Biophysical Journal. 2001; 81:2660–2670. [PubMed: 11606279]

Kam K, Nicoll R. Excitatory synaptic transmission persists independently of the glutamate-glutamine cycle. J Neurosci. 2007; 27:9192–9200. [PubMed: 17715355]

Kash SF, Johnson RS, Tecott LH, Noebels JL, Mayfield RD, Hanahan D, Baekkeskov S. Epilepsy in mice deficient in the 65-kDa isoform of glutamic acid decarboxylase. Proceedings of the National Academy of Sciences of the United States of America. 1997; 94:14060–14065. [PubMed: 9391152]

Liang SL, Carlson GC, Coulter DA. Dynamic regulation of synaptic GABA release by the glutamate-glutamine cycle in hippocampal area CA1. J Neurosci. 2006; 26:8537–8548. [PubMed: 16914680]

Mackenzie B, Schafer MK, Erickson JD, Hediger MA, Weihe E, Varoqui H. Functional properties and cellular distribution of the system A glutamine transporter SNAT1 support specialized roles in central neurons. The Journal of Biological Chemistry. 2003; 278:23720–23730. [PubMed: 12684517]

Mathews GC, Diamond JS. Neuronal glutamate uptake Contributes to GABA synthesis and inhibitory synaptic strength. J Neurosci. 2003; 23:2040–2048. [PubMed: 12657662]

McGale EH, Pye IF, Stonier C, Hutchinson EC, Aber GM. Studies of the inter-relationship between cerebrospinal fluid and plasma amino acid concentrations in normal individuals. Journal of Neurochemistry. 1977; 29:291–297. [PubMed: 886334]

Melone M, Quagliano F, Barbaresi P, Varoqui H, Erickson JD, Conti F. Localization of the glutamine transporter SNAT1 in rat cerebral cortex and neighboring structures, with a note on its localization in human cortex. Cereb Cortex. 2004; 14:562–574. [PubMed: 15054072]

Rae C, Hare N, Bubb WA, McEwan SR, Broer A, McQuillan JA, Balcar VJ, Conigrave AD, Broer S. Inhibition of glutamine transport depletes glutamate and GABA neurotransmitter pools: further evidence for metabolic compartmentation. Journal of Neurochemistry. 2003; 85:503–514. [PubMed: 12675927]

Sepkuty JP, Cohen AS, Eccles C, Rafiq A, Behar K, Ganel R, Coulter DA, Rothstein JD. A neuronal glutamate transporter contributes to neurotransmitter GABA synthesis and epilepsy. J Neurosci. 2002; 22:6372–6379. [PubMed: 12151515]

NIH-PA Author Manuscript

NIH-PA Author Manuscript

NIH-PA Author Manuscript

Solbu TT, Bjorkmo M, Berghuis P, Harkany T, Chaudhry FA. SAT1, A Glutamine Transporter, is Preferentially Expressed in GABAergic Neurons. Front Neuroanat. 2010; 4:1–13. [PubMed: 20161990]

Stafford MM, Brown MN, Mishra P, Stanwood GD, Mathews GC. Glutamate spillover augments GABA synthesis and release from axodendritic synapses in rat hippocampus. Hippocampus. 2010; 20:134–144. [PubMed: 19338018]

Tani H, Bandrowski AE, Parada I, Wynn M, Huguenard JR, Prince DA, Reimer RJ. Modulation of epileptiform activity by glutamine and system A transport in a model of post-traumatic epilepsy. Neurobiology of Disease. 2007; 25:230–238. [PubMed: 17070687]

Varoqui H, Zhu H, Yao D, Ming H, Erickson JD. Cloning and functional identification of a neuronal glutamine transporter. The Journal of Biological Chemistry. 2000; 275:4049–4054. [PubMed: 10660562]

Wang DD, Kriegstein AR. Defining the role of GABA in cortical development. The Journal of Physiology. 2009; 587:1873–1879. [PubMed: 19153158]

Yao D, Mackenzie B, Ming H, Varoqui H, Zhu H, Hediger MA, Erickson JD. A novel system A isoform mediating Na+/neutral amino acid cotransport. The Journal of Biological Chemistry. 2000; 275:22790–22797. [PubMed: 10811809]

Abbreviations

ACSF	artificial cerebrospinal fluid
CA1	cornu ammonis 1
DNQX	6,7-dinitroquinoxaline-2,3-dione
EAAT	excitatory amino acid transporter
GAD	glutamic acid decarboxylase
GAT-1	GABA reuptake transporter
MeAIB	α-(methyl-amino) isobutyric acid
mIPSC	miniature inhibitory postsynaptic current
MK-801	dizocilpine maleate
3-MPA	3-mercaptoproprionic acid
SNAT	sodium-coupled neutral amino acid transporter
TPMPA	(1,2,5,6-Tetrahydropyridin-4-yl) methylphosphinic acid hydrate
TTX	tetrodotoxin
vGAT	vesicular GABA transporter

NIH-PA Author Manuscript
NIH-PA Author Manuscript
NIH-PA Author Manuscript

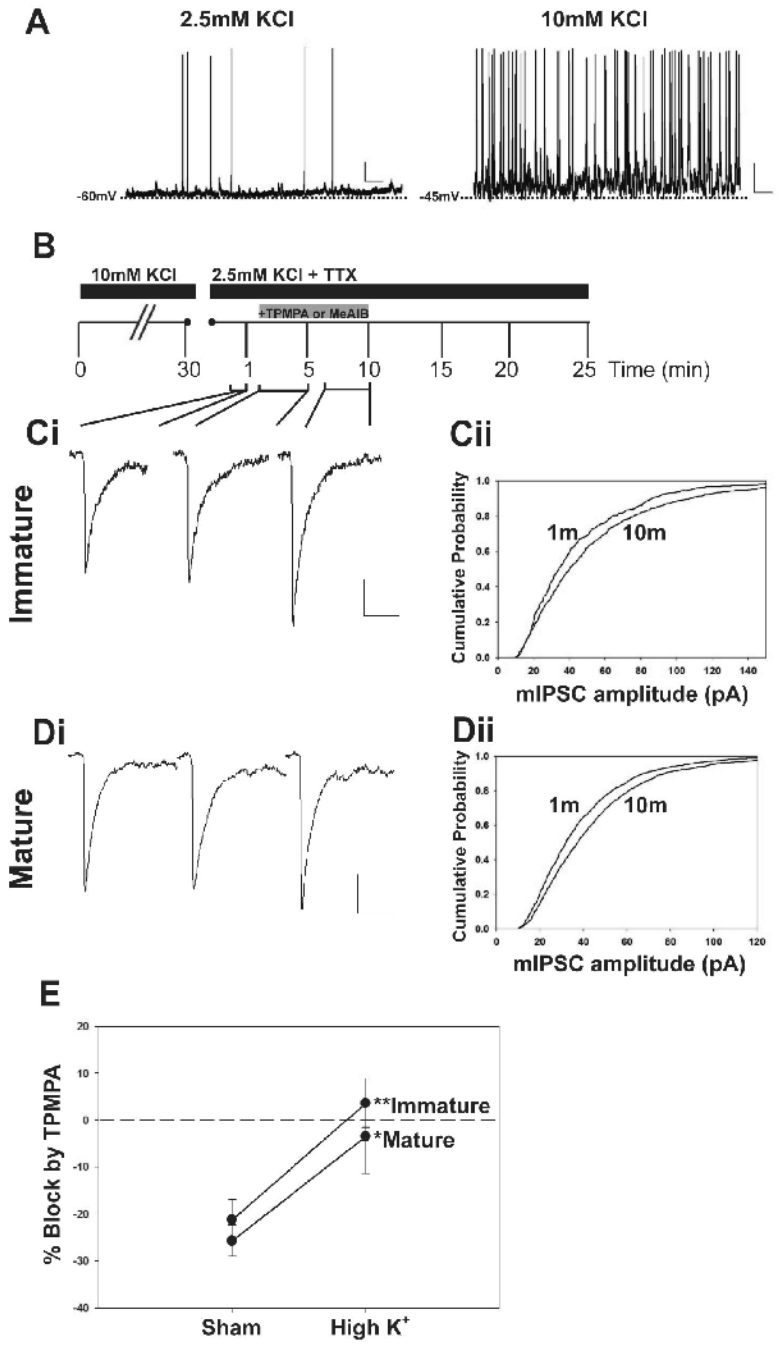

Figure 1. System A-dependent increase in quantal size and synaptic cleft GABA concentration after a hyperexcitable period

A, Representative action potential and spontaneous postsynaptic potential waveforms recorded from an immature CA1 pyramidal neuron during sham-treatment (2.5mmol/L KCl) or high K^+-induced depolarization (10mmol/L KCl). Scale bars represent 10mV and 1s. **B,** Time line of experimental protocol for high K^+-induced depolarization of hippocampal slices. During the first segment, slices were exposed to high K+ for approximately 30 minutes, which included transfer to the recording chamber and recording a period of spontaneous activity. The second segment represents the time elapsed following the end of the exposure to high K^+. **Ci, Di,** Representative averaged mIPSC waveforms at 1, 5, and 10

NIH-PA Author Manuscript

NIH-PA Author Manuscript

NIH-PA Author Manuscript

minutes following high K^+-induced depolarization. Scale bars, 10pA and 20ms. **Cii, Dii,** Cumulative probability histograms (n=7) of mIPSC amplitudes measured at 1 and 10 minutes following high K^+-induced depolarization of slices from immature (C) and mature (D) rats. **E,** Comparison of the effect of TPMPA on mIPSC amplitudes reported as % block by TPMPA following sham-treatment or high K^+-induced depolarization. The % block was determined by calculating the % change in mIPSC amplitudes at ten minutes compared with mIPSC amplitudes recorded within the first minute following high K^+. Immature, P8-12; Mature, P21-28. See text for 'n'; Error bars, SEM.

NIH-PA Author Manuscript
NIH-PA Author Manuscript
NIH-PA Author Manuscript

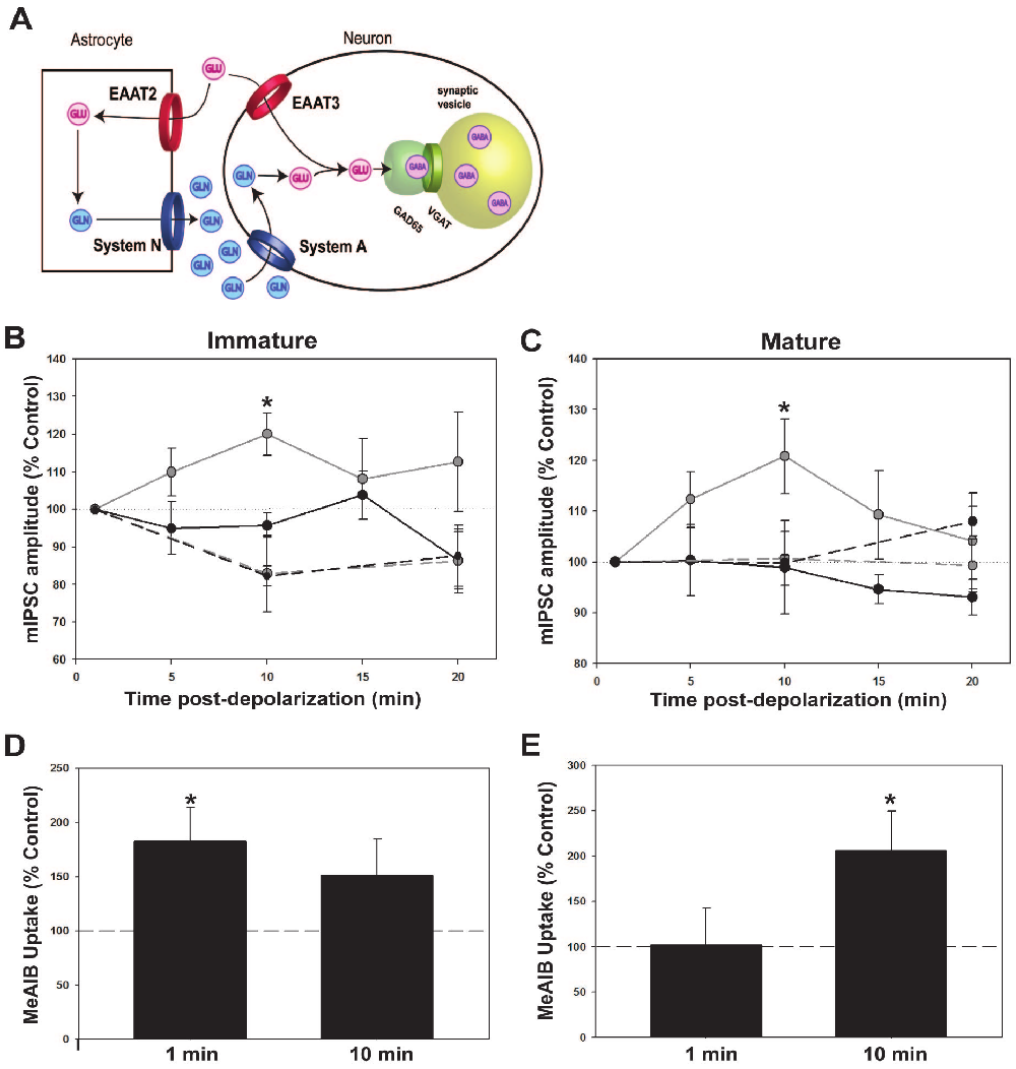

Figure 2. Depolarization augments inhibitory synaptic strength in a System A-dependent manner and increases System A activity on synaptosomes

A, Schematic illustration of GABA biosynthetic pathways. GAD65 and the vesicular GABA transporter (vGAT) are part of a complex of proteins that link GABA synthesis and vesicular filling. Neurons acquire glutamate through direct uptake by EAAT3 or through the glutamate-glutamine-GABA pathway. In this pathway, astrocytes uptake glutamate via EAAT2, convert it to glutamine, and export glutamine via System N transporters for neuronal uptake by System A transporters. Neurons convert glutamine back to glutamate. **B, C,** Time course displaying the % of control mIPSC amplitudes across time following sham treatment (black) or high K^+-induced depolarization (gray) corresponding to the second segment in Fig 1B. MeAIB was washed-in between minutes 2-7 and its effect was assessed at ten minutes in control cells (black dashed) or following high potassium (gray dashed). The % of control mIPSC amplitude was calculated by normalizing the average median mIPSC amplitudes at each reported timepoint to the mIPSC amplitude at 1 minute. **D, E,** Comparison of [^{3}H]MeAIB uptake reported as % of control at 1 or 10 minutes after high K^+-induced depolarization. **A-D,** See text for 'n', *p<0.05; Error bars, SEM. Immature, P8-12; Mature P21-28.

NIH-PA Author Manuscript
NIH-PA Author Manuscript
NIH-PA Author Manuscript

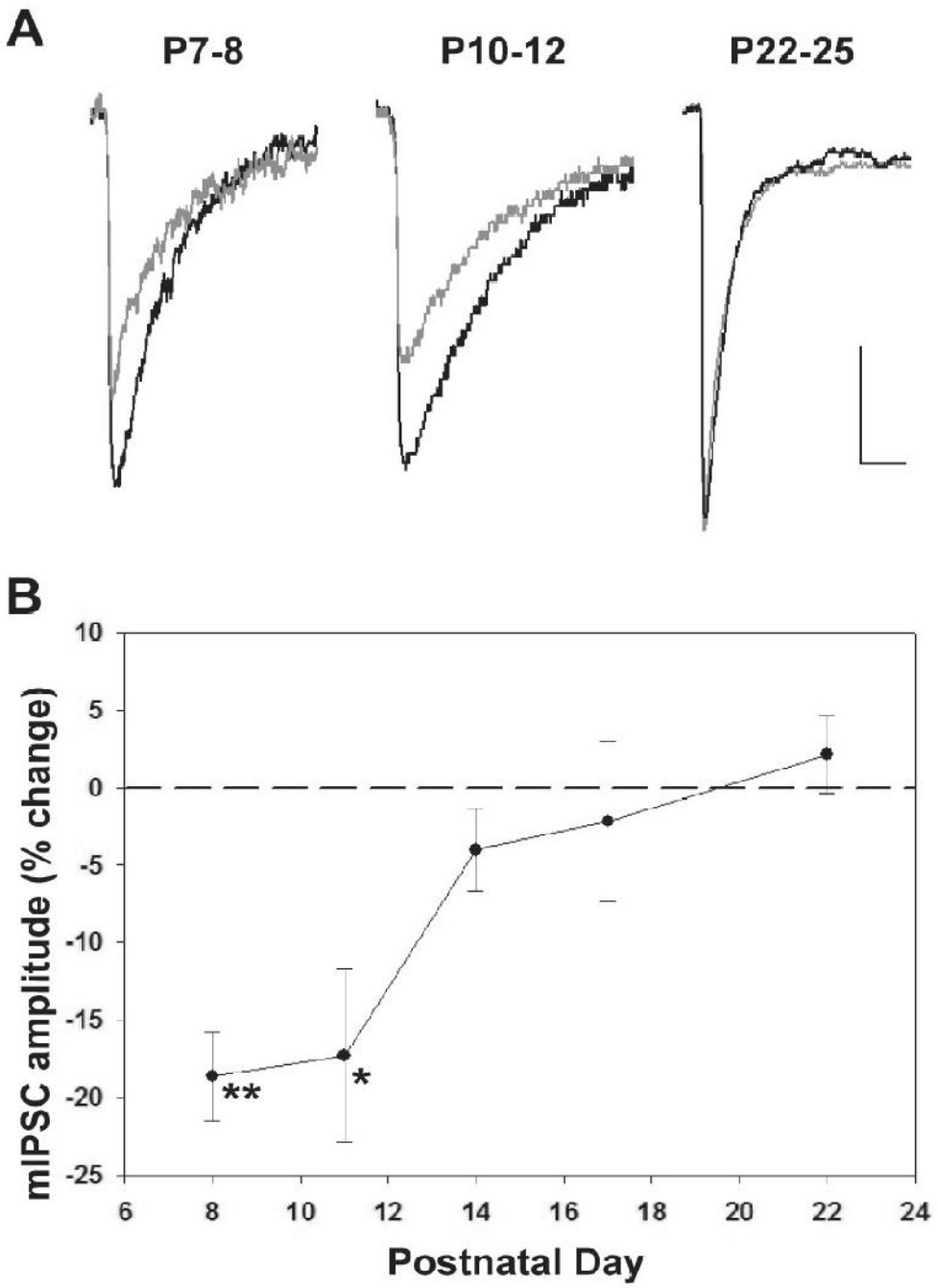

Figure 3. The constitutive contribution of System A-mediated glutamine uptake to vesicular GABA content decreases during maturation

A, Average mIPSC waveforms from a representative cell in control (black) and after 5 minutes in 10mmol/L MeAIB at sequential postnatal ages. Scale bars, 10pA and 20ms. **B,** Plot demonstrating the age-dependent effect of MeAIB on mIPSC amplitudes. Each point represents the average percent change from baseline across a range of postnatal ages (n=7) (see Suppl. Table 1). **p<0.01, *p<0.05; Error bars, SEM.

NIH-PA Author Manuscript
NIH-PA Author Manuscript
NIH-PA Author Manuscript

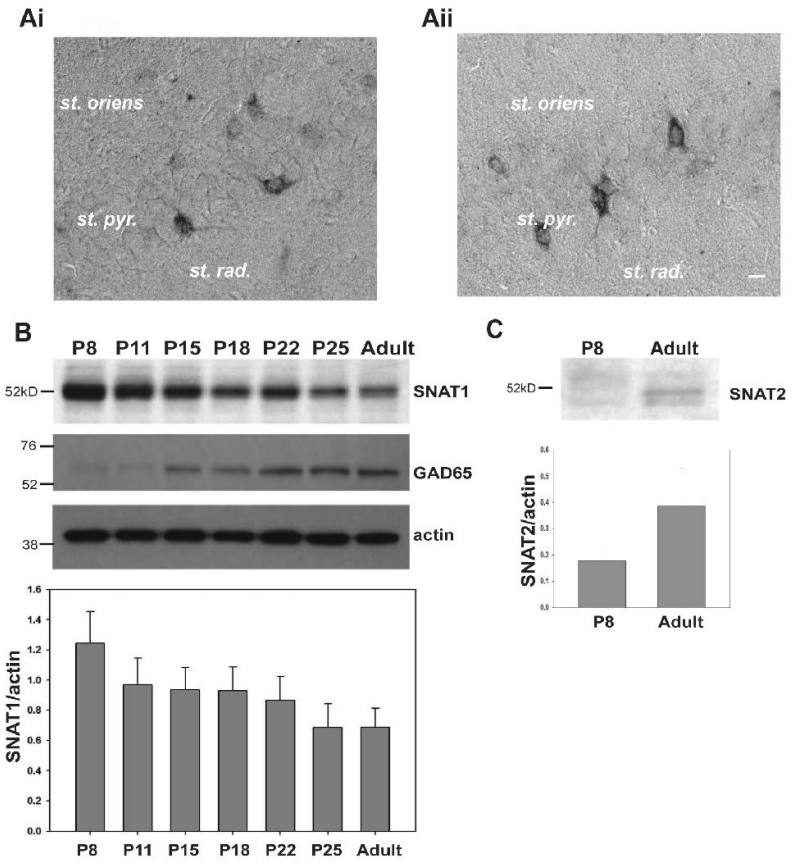

Figure 4. SNAT1 expression in hippocampus decreases with postnatal maturation

Ai-ii, Non-pyramidal cell bodies localized in *stratum oriens* (*st. oriens*), *st. radiatum* (*st. rad.*) and bordering *stratum pyramidale* (*st. pyr.*) in both immature (Ai; P8) and mature (Aii; P25) hippocampus positively express SNAT1. Scale bar represents 20μm. **B, C,** Representative western blots illustrating amount of SNAT1, GAD65 and SNAT2 expressed in whole hippocampal lysates from sequential postnatal ages and adulthood. Actin was used as a loading control. Bar graphs compare SNAT1 and SNAT2 protein levels after normalization to actin (n=3; SNAT1/actin v. time, $p<0.001$, Spearman's Rank Order Correlation Test). The position of protein standards is shown on the left. Error bars, SEM.

NIH-PA Author Manuscript

NIH-PA Author Manuscript

NIH-PA Author Manuscript

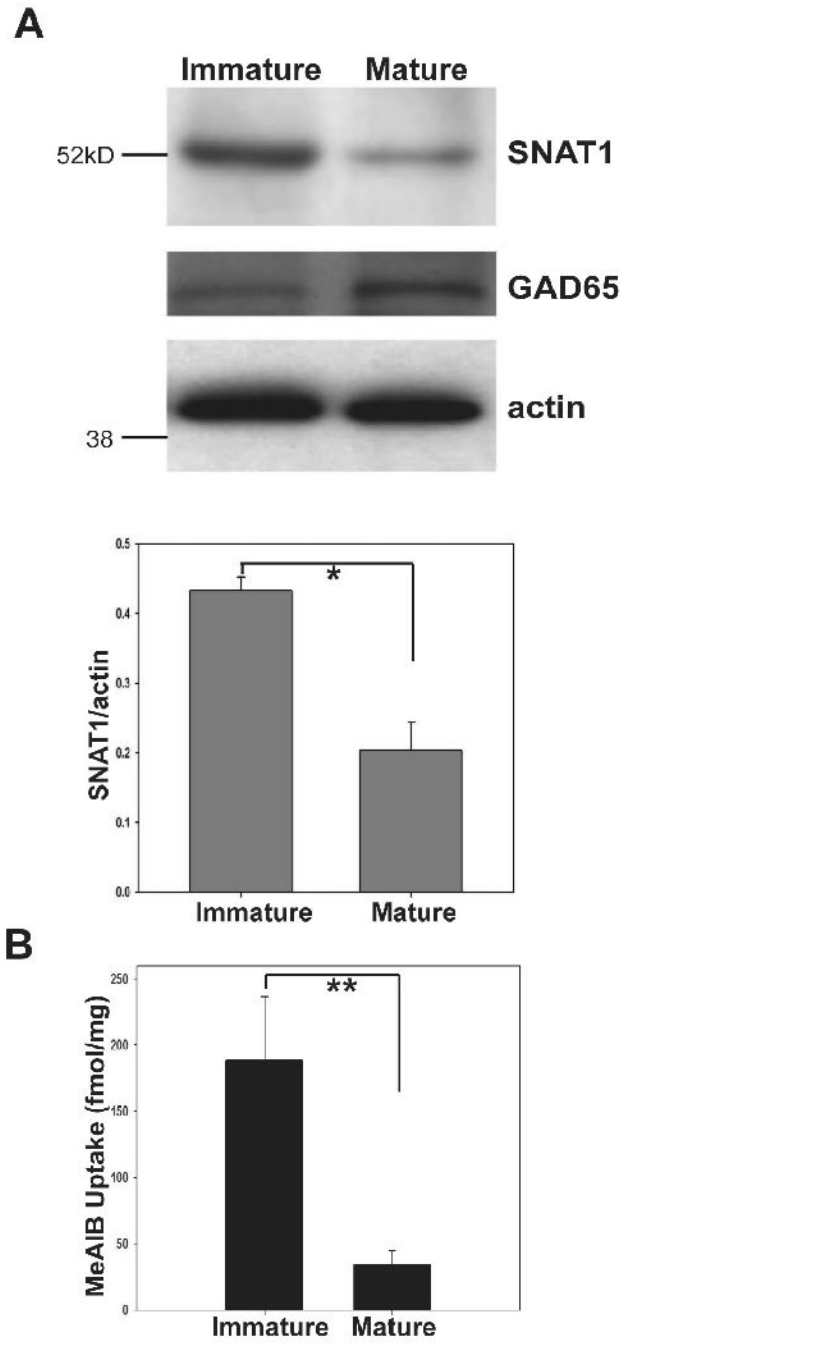

Figure 5. Reduced SNAT1 activity at mature synaptic membranes correlates with loss of System A's constitutive contribution to synaptic GABA

A, Representative western blots illustrating amount of SNAT1 and GAD65 protein expressed in immature and mature hippocampal synaptosomes. The position of protein standards is shown on the left. Actin served as a loading control. Bar graph compares SNAT1 levels after normalization to actin (n=3), **p<0.01. **B,** Comparison of MeAIB uptake reported as fmol/mg protein between immature (P8-12) and mature (P21-28) hippocampal synaptosomes (n=3), *p<0.05. **B-C,** Error bars, SEM.

NIH-PA Author Manuscript

NIH-PA Author Manuscript

NIH-PA Author Manuscript

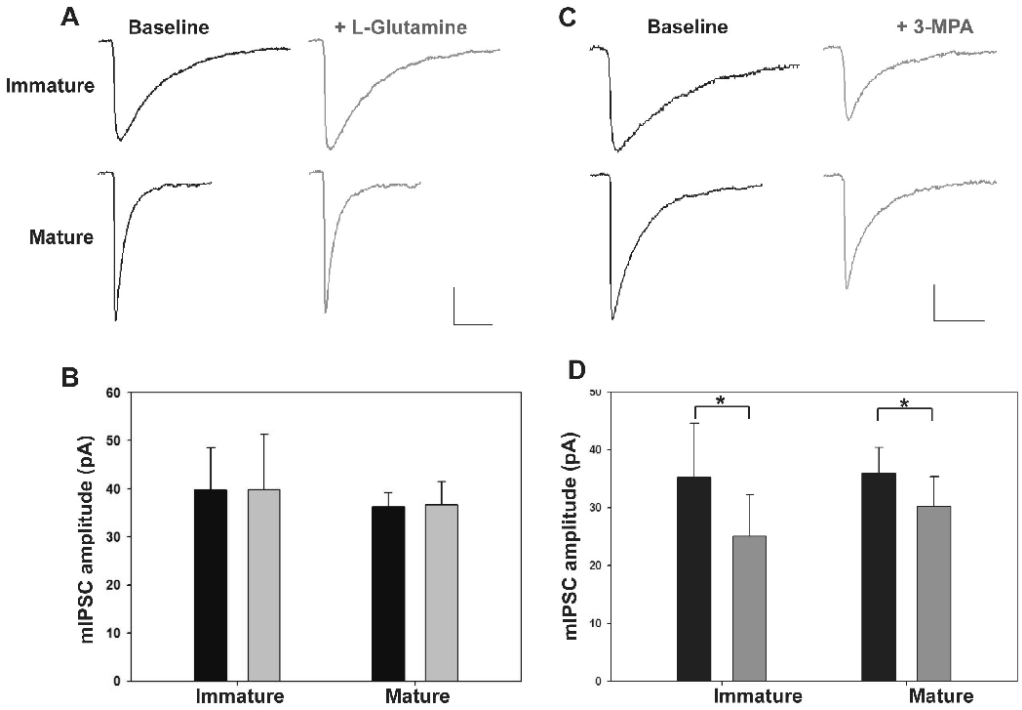

Figure 6. Changes in glutamine supply and new GABA synthesis do not account for maturational loss of glutamine's contribution to vesicle filling

A, Representative average mIPSC waveforms in control (black) and after 5 min. in exogenous 2mM glutamine from immature and mature slices. **B,** Comparison of the effect of 2mmol/L exogenous glutamine reported as a percent control of baseline (n=5). Error bars, SEM. **C,** Average representative mIPSC waveforms from control (black) neurons and neurons exposed to 1mmol/L 3-MPA in immature and mature slices. **D,** Comparison of mIPSC amplitudes in control (black) and in 1mmol/L 3-MPA ACSF (see text for 'n') reported as average median mIPSC amplitudes. *p<0.05; Error bars, SD. **A, C,** Scale bars, 10pA and 20ms. Immature, P8-12; Mature, P21-28.